High temperature mechanical strength and microstructural stability of advanced 9-12%Cr steels and ODS steels.

B. Fournier,[1] M. Salvi[1], C. Caës[1], J. Malaplate[1], F. Dalle[1], M. Sauzay[1], Y. de Carlan[1], A. Pineau[2]

[1] CEA Saclay, DEN/DANS/DMN/SRMA, 91191 Gif sur Yvette Cedex, France;

[2] ENSMP, Centre des Matériaux P.-M. Fourt, UMR CNRS 7633, BP 87, 91003 Evry, France;

E-mail: *benjamin.fournier@cea.fr*

1. Abstract

The present study proposes a comparison between several martensitic and ferritic steels in terms of creep strength and cyclic softening effect. The damage mechanisms are identified using fractographic observations and the microstructural evolutions are observed by TEM. The effects of a modified chemical composition on the high temperature mechanical behaviour are studied.

2. Introduction.

In the framework of Generation IV nuclear reactors and for fusion reactors, oxide dispersion strengthened (ODS) steels and advanced generations of 9-12%Cr martensitic steels are widely investigated [1-4]. Several components in these concepts will be subjected to mechanical loadings (creep, creep-fatigue,...) at high temperatures, between 550°C and 650°C. A high creep strength coupled to an improved microstructural stability during deformation are two key properties for such applications.

The creep strength of the standard commercial steels (typically P91) is derived from the materials properties in the as-received conditions for such applications. However, recent studies [5-8] have shown that the microstructural evolutions that occur during cyclic loading (subgrain coarsening and decrease of the dislocations density) can lead to a drastic deterioration of the creep strength (the minimum creep rate can be 100 times faster). Under the combined creep-fatigue loading condition, the microstructural stability of conventional 9-12%Cr steels is therefore a key issue.

In the present article advanced 9-12%Cr steels, including their ODS grades, are tested under creep, fatigue and creep-fatigue conditions. The mechanical tests results, as well as the optical, SEM and TEM observations are reported. These results are finally discussed in terms of deformation mechanisms and lifetime prediction [9].

3. Materials and mechanical tests.

Four different steels were tested in the present study:

1) A commercial martensitic P92 steel produced by Vallourec Mannesmann.
2) and 3) Two laboratory martensitic steels reinforced with either 0.007% of boron (B-added VY2 steel) or 0.2% of titanium (Ti-added Ti1 steel) steel produced by Aubert & Duval. Both materials were austenitized at 1200°C for 30min and tempered at 720°C for 10h.

4) A ferritic ODS steel containing 14%Cr and 0.3% of Y_2O_3 obtained by powder metallurgy and hot extrusion process at CEA Saclay.

Creep tests were carried out both at 550°C and 650°C for B-added and Ti-added steels (see table 1) and the results obtained compared with those published for P92 and ODS steels. Fatigue and creep-fatigue tests were carried out at 550°C on these four materials. More details about these specific testing procedures and the TEM examinations can be found in [6,10].

Material	Stress (MPa)	T (°C)	Status	Lifetime (h)	Minimum creep rate (h^{-1})
Ti-added	235	550	broken	253	$1.88x10^{-4}$
Ti-added	235	550	broken	137	$2.49x10^{-4}$
B-added	235	550	broken	197	$2.63x10^{-4}$
B-added	235	550	broken	274	$2.46x10^{-4}$
Ti-added	90	650	unbroken	>2260	$<5.38x10^{-7}$
B-added	90	650	unbroken	>1700	$<2.27x10^{-5}$
Ti-added	200	550	unbroken	>2185	$<2.55x10^{-6}$
Ti-added	60	650	unbroken	>2067	$<2.00x10^{-7}$
B-added	60	650	unbroken	>2156	$<3.31x10^{-6}$

Table 1 - Creep tests carried out on VY2 and Ti1 materials.

4. Results

4.1. Creep tests

ODS steels are known to present a much higher creep strength at high temperature than conventional martensitic steels [11]. However, the creep properties of conventional martensitic steels have been continuously improving [12-13] and constant efforts are still being made to improve their creep strength. The better creep strength of steel P92 compared to steel P91 has already been reported and tabulated [14]. Figure 1 presents the results of short time creep tests carried out at 550°C on B-added and Ti-added steels compared to P91 at 235MPa. At this temperature and for such high stresses, where creep is mainly driven by dislocation glide, B-added and Ti-added steels present a much poorer creep strength than conventional P91. However, in figure 2, results of two currently

running tests carried out at 650°C and at 90MPa are presented. For this loading the creep lifetime of P91 is around 1000h (as shown in figure 2) compared to around 9000h for P92. Under these conditions the behaviour of the B-added steel is somewhat better than P91, while that of the Ti-added steel can be expected to be just as good as P92 if not better.

4.2 Fatigue and creep-fatigue tests

Figure 3a presents the pure fatigue lifetime of P91, P92, B-added, Ti-added and the ODS steel expressed in terms of the plastic strain range applied at 550°C. All these tests were done under the total strain control. P91 and P92 present very similar lifetimes, whereas, the Ti-added and B-added steels are significantly less resistant. Finally, the 14%Cr ODS steel is the least resistant to fatigue for a given applied plastic strain. However this test was carried out at the same total strain than those on B-added and Ti-added steels, the much higher yield stress of the ODS steel explains the very low plastic strain applied. And expressed in terms of the total strain applied, the ODS steel presents a lifetime as good as P91 or P92 and better than B-added and Ti-added steels (figure 3b).

Figure 4 presents the variations of the stress range during cycling for pure fatigue and creep-fatigue tests carried out on P91, B-added, Ti-added and the ODS steel. In addition to having a shorter lifetime than P91, B-added and Ti-added steels, these steels also present a stronger and faster cyclic softening effect. This softening effect is even more pronounced under creep-fatigue loading than under fatigue loading, which is not the case for P91 under the same conditions. On the contrary, the ODS steel shows a good stability (neither softening nor hardening) of the measured stress until final fracture.

Figure 5 shows SEM and optical observations on B-added steel after pure fatigue ($\Delta\varepsilon_{fat}$ = 0.7%) and creep-fatigue ($\Delta\varepsilon_{fat}$ = 0.7% and ε_{creep} = 0.5%) tests. These observations are representative of both B-added and Ti-added materials. They confirm the fact that two types of damage occur, depending on the loading, as previously identified on P91 steel [10]. Indeed, for low applied strains, cracks are narrow and highly branched, whereas for higher applied strains, cracks are much wider, completely filled with oxide. In addition in the second case, cracks seem to initiate through the brittle fracture of the oxide scale.

Figure 6 presents TEM observations of the B-added steel in the as-received conditions, after pure fatigue and after creep-fatigue. As previously observed on P91 steel, the initial martensitic microstructure is unstable (subgrain coarsening, decrease of the dislocations density) under cyclic loading and this is correlated to the cyclic softening effect [5]. However, in the present case, the initial subgrain size is significantly smaller than that of P91. In addition, although TEM measurements were not carried out on the P91 sample tested in pure fatigue at $\Delta\varepsilon_{fat}$ = 0.7%, other measurements show that the mean subgrain size should be between 0.7 and 1.1µm. That is, the subgrain size after fatigue is smaller than

after creep-fatigue. Surprisingly enough, for B-added and Ti-added, this is not true: pure fatigue leads to a larger subgrain size than creep-fatigue (table 2). No significant precipitate coarsening was measured.

	As received material	After fatigue ($\Delta\varepsilon_{fat}$ = 0,7%)	After creep-fatigue ($\Delta\varepsilon_{fat}$ = 0,7% and ε_{creep} = 0,5%)
B-added	0.12	1.07	0.54
Ti-added	0.085	1.27	1.06
P91	0.37	NA	1.1

Table 2 - mean subgrain size (in µm) measured on P91, Ti-added and B-added steels from TEM observations on several specimens. The number of analysed grains varies between: 500 and 5000.

5. Discussion

The present results clearly show that reinforcement with boron or titanium (B-added and Ti-added steels) does not lead to an improvement in creep or fatigue at 550°C. However, this might be due to heat treatments that were not optimized for these first trials. The most negative point is that the microstructure is found to be even more unstable than for P91 or P92 steels. Indeed, if the subgrain size after loading is comparable to that measured on P91, the ratio between this final subgrain size and the initial one is much higher. Such increased instability is coherent with the more pronounced softening effect reported in figure 4. At 650°C, on the contrary, the creep behaviour of these steels is very promising.

This difference in behaviour at between these two temperatures can probably be explained in terms of the deformation mechanisms. Indeed, at 550°C, the deformation mechanism is mainly driven by dislocation glide, whereas, at 650°C, the applied stresses are much lower and the controlling mechanism should be linked to diffusion processes. This suggests that the precipitates present in B-added and Ti-added steels are more stable at high temperature than those of P91, leading to a better creep resistance when diffusion and precipitate stability are involved. However, the heat treatments applied do not enable to obtain a stable martensitic microstructure, which is then easily modified by dislocation glide at 550°C.

These results show that both the chemical composition and the heat treatments must be optimized to improve both the cyclic and the creep behaviour. Depending on the loading temperature, the deformation mechanisms are modified. Therefore, obtaining a stable precipitation state (necessary when diffusion processes are involved) is not enough. Stabilizing the subgrain boundaries is also a major issue.

In addition, in terms of fatigue lifetime, B-added and Ti-added steels exhibit a significantly shorter lifetime than P91 and P92 steels. However, the damage mechanisms seem quite similar. In a previous study [9] a lifetime prediction model was proposed. In this model, the number of cycles to crack initiation is calculated using the Tanaka and Mura [15] formula. This number of cycles to crack initiation is inversely proportional to the grain diameter. For P91, the grain diameter was around 20µm, whereas for Ti-added and B-added steels, the grain diameter is close to 300µm, which means that the number of cycles to crack

initiation is about 10 times lower than for the P91 steel. This grain size effect seems to be the reason for the shorter fatigue lifetimes observed on Ti-added and B-added steels.

On the contrary, the ODS steel tested here, presents a very stable behaviour even under cyclic loading as previously shown on 9%Cr ODS steel [16]. This is quite promising for creep-fatigue design since no microstructural evolution occurs. Therefore, the mechanical behaviour measured in the as-received state still applies all along the lifetime, contrary to 9-12%Cr steels.

6. Conclusions

Creep, fatigue and creep-fatigue tests were carried out on several 9-12%Cr steels and a 14%Cr ODS steel. Two laboratory produced steels, reinforced with either boron or titanium, were also tested.

The results obtained show that precipitates formed in boron or titanium modified heats are more stable during high temperature (650°C) creep than in P91. However at lower temperatures (550°C), where, dislocation glide and the stability of subgrain boundaries are the main deformation controlling mechanisms, these two steels are less stable and present shorter lifetimes than P91. This is probably due to inadequate heat treatment used that lead to a much finer initial microstructure (subgrain size three times smaller than for P91).

The ODS steel proved to be more stable under cyclic deformation, in addition to having a much better creep strength.

7. Acknowledgements

This work was carried out at the Nuclear Energy division of CEA with the support of the DDIN/RSP project.

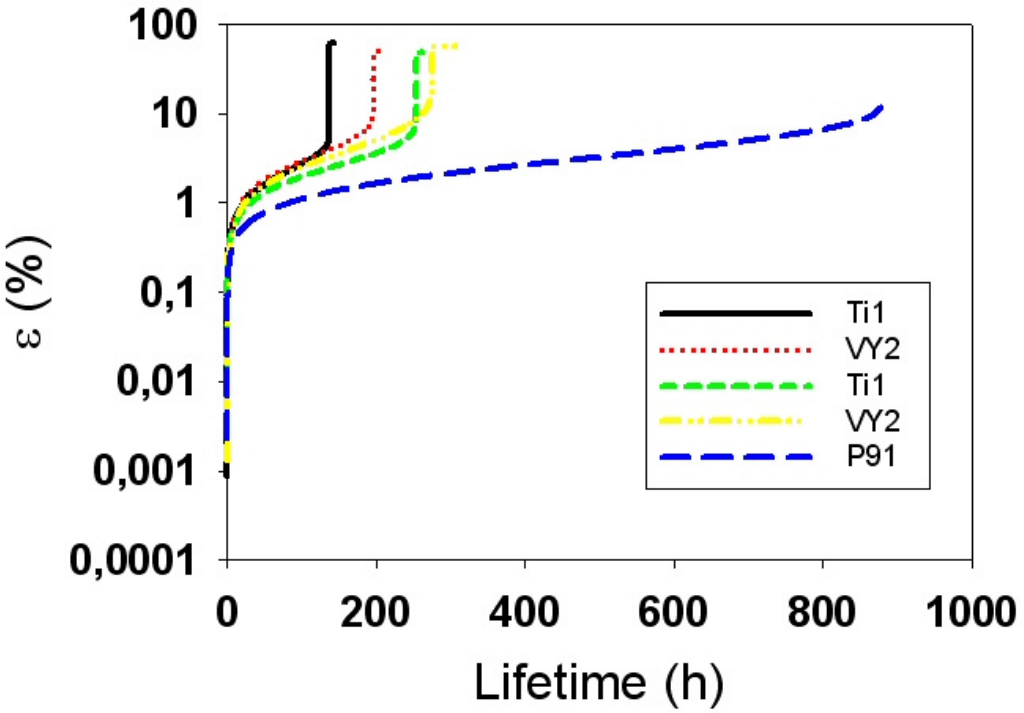

Figure 1 - Creep curves on Ti-added and B-added steels compared to P91 (550°C and 235MPa).

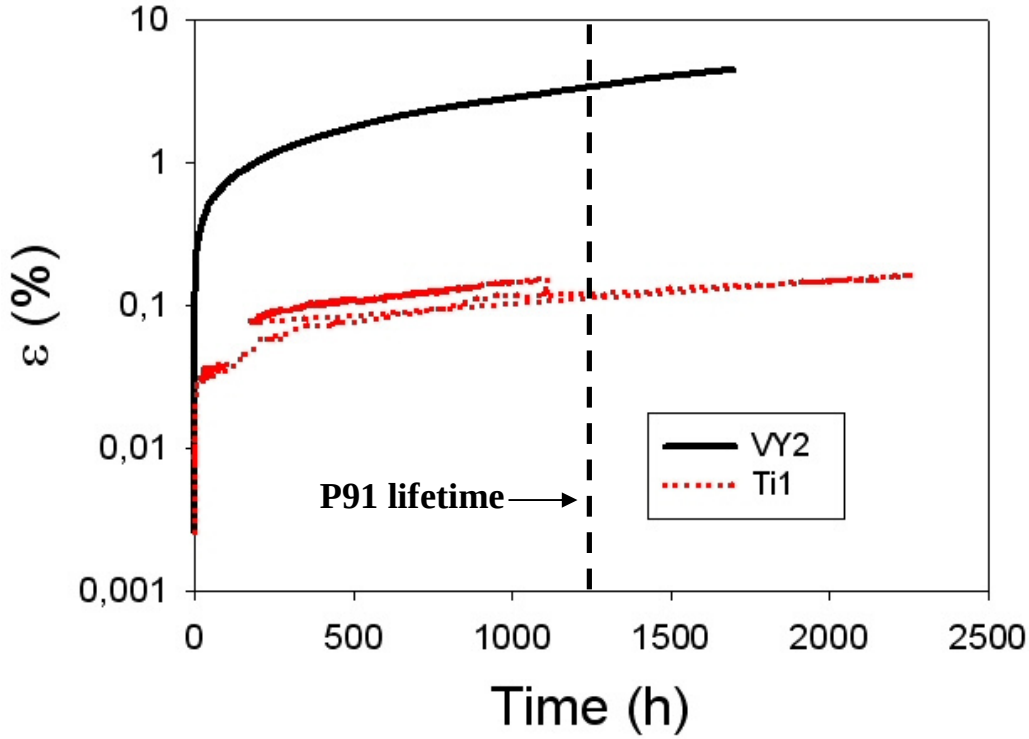

Figure 2 - Creep curves of Ti-added and B-added steels at 650°C and at 90MPa. Tests are still running.

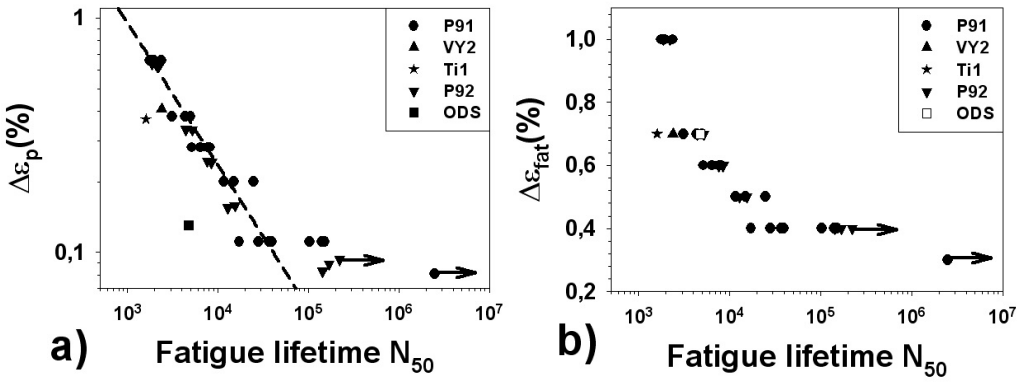

Figure 3 - Pure fatigue lifetime for P91, P92, Ti-added, B-added and a 14%Cr ODS steel at 550°C expressed in terms of the plastic strain range applied.

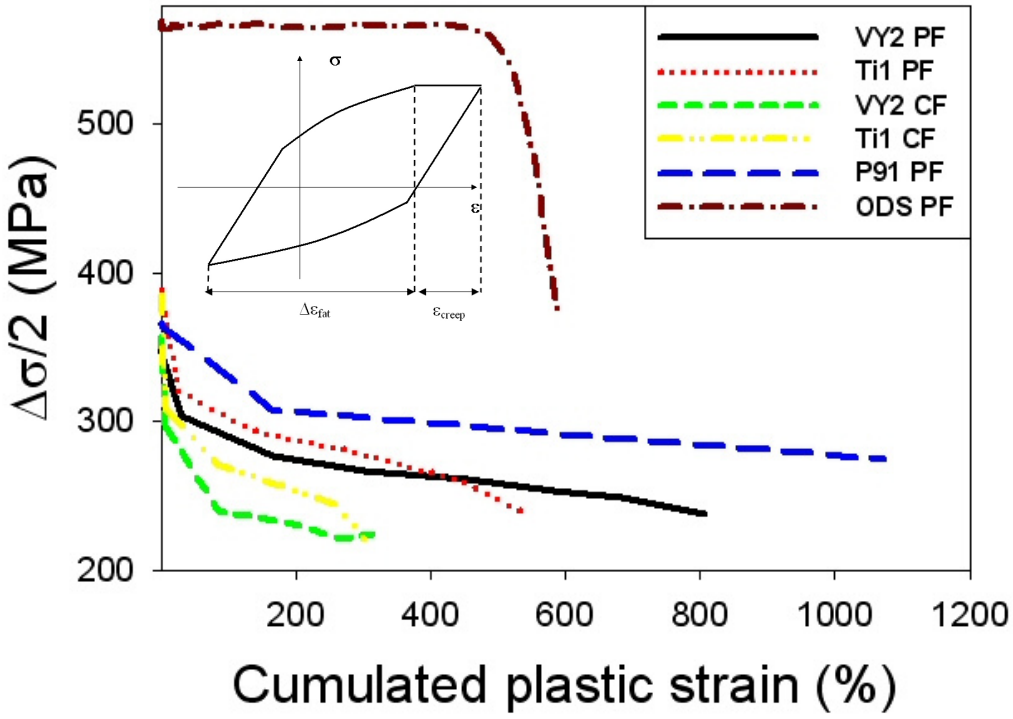

Figure 4 - Stress evolution under pure fatigue (PF : $\Delta\varepsilon_{fat}$ = 0.7%) and creep-fatigue (CF : $\Delta\varepsilon_{fat}$ = 0.7% and ε_{creep} = 0.5%) loadings at 550°C.

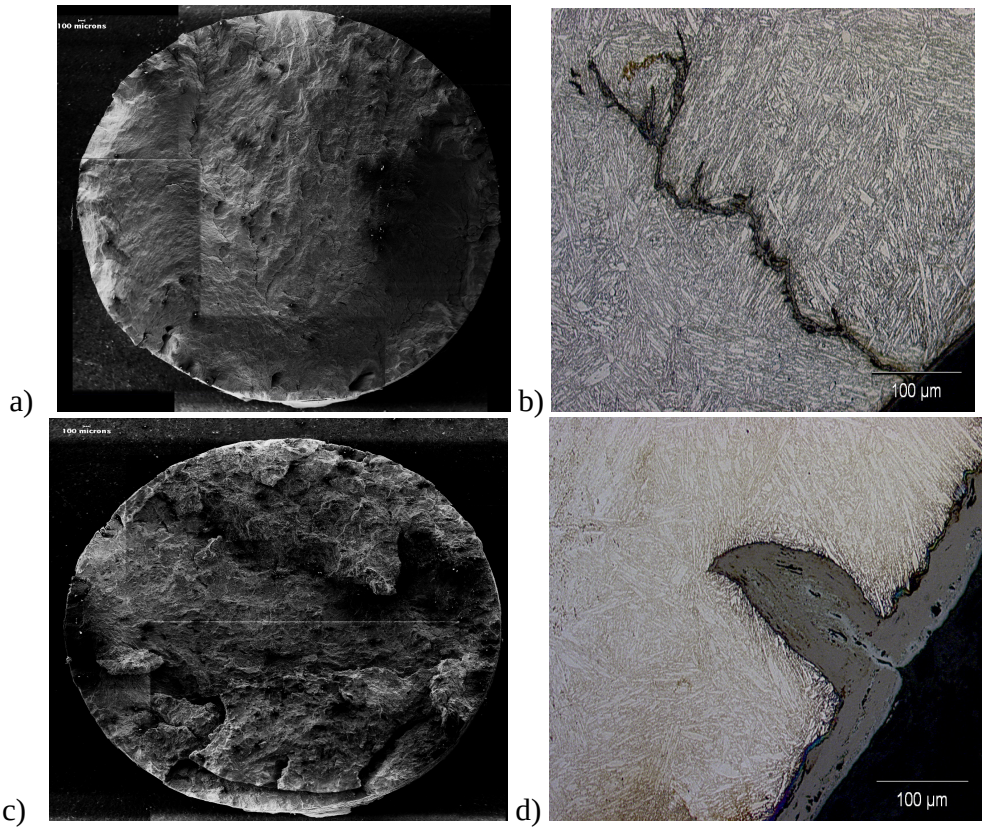

Figure 5 - SEM fractographic (a and c) and optical (b and d) micrographsof the cross sections of B-added steel after (a and b) pure fatigue loading and (c and d) creep-fatigue loading.

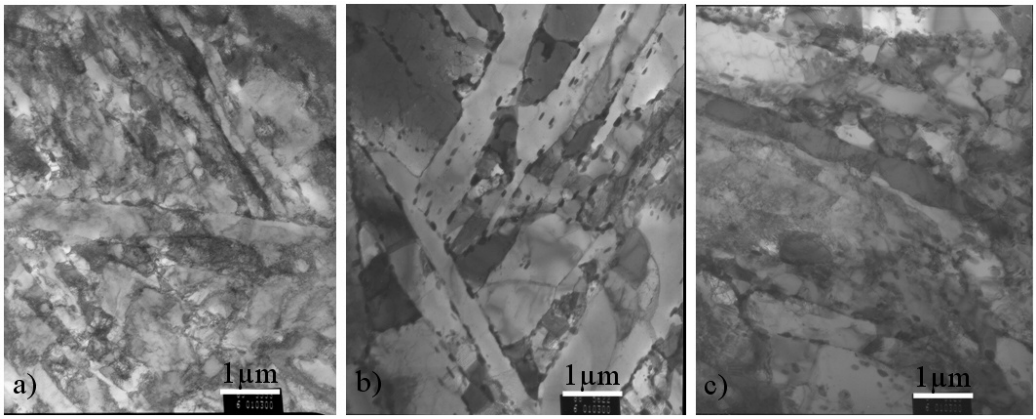

Figure 6- Bright field TEM observations of B-added a) in the as-received condition, b) after pure fatigue loading and c) after creep-fatigue loading.

References

[1] R.W. Swindeman, M.L. Santella, P.J. Maziasz, B.W. Roberts, K. Coleman. Issues in replacing Cr-Mo steels and stainless steels with 9Cr-1Mo-V steel. Pressure Vessels and Piping 81, 507-512, 2004.
[2]R. Klueh and D. Harries, High chromium ferritic and martensitic steels for nuclear applications, ASTM, USA, 2001.
[3] D. Iracane, H.A. Abderrahim, F. Carré, P. Chaix, J.L. Séran, P. Yvon, Generation IV systems R&D needs and research reactors policy, IAEA Technical committee meeting on "research reactors support needed for innovative nuclear power reactors and fuel cycles", Vienna, Austria, November 20th to 22nd, 2006.
[4] Y. de Carlan, CEA Development Of New Ferritic ODS Alloys For Nuclear Application, ICFRM13, Nice, France, 2007.
[5] B. Fournier, M. Sauzay, C. Caës, M. Noblecourt, M. Mottot, L. Allais, I. Tournié, A. Pineau, Creep-fatigue interactions in a 9%Cr-1%Mo martensitic steel - Part I: mechanical tests results, Accepted by Materials and Metallurgical Transactions, 2008.
[6] B. Fournier M. Sauzay, F. Barcelo, E. Rauch, A. Renault, T. Cozzika, L. Dupuy, A. Pineau, Creep-fatigue interactions in a 9%Cr-1%Mo martensitic steel - Part II: microstructural evolutions, Accepted by Materials and Metallurgical Transactions, 2008.
[7] B. Fournier, Fatigue-Fluage des aciers martensitiques à 9-12%Cr : comportement et endommagement, PhD Thesis, Ecole des Mines de Paris, 2007.
[8] J.S. Dubey, H. Chilukuru, J.K. Chakravartty, M. Schwienheer, A. Scholz, and W. Blum. Effects of cyclic deformation on subgrain evolution and creep in 9-12%Cr-steels. Materials Science & Engineering A, 406:152_159, 2005.
[9] B. Fournier M. Sauzay, C. Caës, M. Noblecourt, M. Mottot, A. Bougault, V. Rabeau, J. Man, O. Gillia, P. Lemoine, A. Pineau., Creep–fatigue–oxidation interactions in a 9Cr–1Mo martensitic steel. Part III: Lifetime prediction, International Journal of Fatigue, 30, 1797-1812, 2008
[10] B. Fournier M. Sauzay, C. Caës, M. Noblecourt, M. Mottot, A. Bougault, V. Rabeau, A. Pineau,, Creep–fatigue–oxidation interactions in a 9Cr–1Mo martensitic steel. Part I: Effect of tensile holding periods on fatigue lifetime, International Journal of Fatigue, 30, 649-662, 2008
[11] R. Lindau et al., Fusion Engineering and Design, 75-79, 989-996, 2005
[12] F. Masuyama and T. Yokoyama, New steels for advanced plant up to 620°C, pages 30–44. E. Metcalfe, EPRI, USA, 1995.
[13] L. Korcakova, Microstructure evolution in high strength steel for power plant application : microscopy and modelling. PhD thesis, Technical University of Denmark, 2002.
[14] ECCC data sheets 2005 available at http://www.ommi.co.uk/etd/eccc/advancedcreep/DSheets05ax.pdf
[15] Tanaka K, Mura T. A dislocation model for fatigue crack initiation. J Appl Mech 48:97–103, 1981

[16] Ukai, S. and Ohtsuka, S., Low cycle fatigue properties of ODS ferritic-martensitic steels at high temperature, Journal of Nuclear Materials, 367-370, 234-238, 2007